Confronting Uncertainties of Simulated Air Pollution Concentrations during Persistent Cold Air Pool Events in the Salt Lake Valley, Utah

Xia Sun[1,2*], Cesunica E. Ivey[3], Kirk R. Baker[4], Athanasios Nenes[5,6], Neil P. Lareau[7], Heather A. Holmes[8]

1. *Cooperative Institute for Research in Environmental Sciences, University of Colorado, Boulder, CO 80309, United States*
2. *NOAA Global Systems Laboratory, Boulder, CO 80305, United States*
3. *Civil and Environmental Engineering University of California, Berkeley, CA 94720, United States*
4. *U.S. Environmental Protection Agency, Research Triangle Park, NC 27703, United States*
5. *Institute for Chemical Engineering Sciences, Foundation for Research and Technology Hellas, Patras, GR-26504, Greece*
6. *School of Architecture, Civil & Environmental Engineering, Ecole Polytechnique Fédérale de Lausanne, CH-1015, Lausanne, Switzerland*
7. *Atmospheric Sciences Program, Department of Physics, University of Nevada, Reno, NV 89557, United States*
8. *Department of Chemical Engineering, University of Utah, Salt Lake City, UT 84112, United States*

Abstract: Air pollutant accumulations during wintertime persistent cold air pool (PCAP) events in mountain valleys are of great concern for public health worldwide. Uncertainties associated with the simulated meteorology under stable conditions over complex terrain hinder realistic simulations of air quality using chemical transport models. We use the Community Multiscale Air Quality (CMAQ) model to simulate the gaseous and particulate species for one-month in January 2011 during the Persistent Cold Air Pool Study (PCAPS) in the Salt Lake Valley (SLV), Utah (USA). Results indicate that the temporal variability associated with the elevated NO_x and $PM_{2.5}$ concentrations during PCAP events were captured by the model (r=0.20 for NO_x and r=0.49 for $PM_{2.5}$). However, concentrations were not at the correct magnitude (NMB= -35%/12% for $PM_{2.5}$ during PCAPs/non-PCAPs) where $PM_{2.5}$ was underestimated during PCAP events and overestimated during non-PCAP periods. The underestimated PCAP strength is represented by valley heat deficit, which contributed to the underestimated $PM_{2.5}$ concentrations compared with observations due to the model simulating more vertical mixing and less stable stratification than what was observed. Based on observations, the dominant $PM_{2.5}$ species were ammonium and nitrate. We provide a discussion that aims to investigate the emissions and chemistry model uncertainties using the nitrogen ratio method and the thermodynamic ammonium nitrate regime method.

**Corresponding author*: xia.sun@noaa.gov

Keywords: Chemical Transport Model; CMAQ; WRF; evaluation; air quality; temperature inversion; PCAP

Synopsis

We investigate air quality model uncertainties related to meteorology and chemistry for wintertime air pollution episodes in the mountainous western United States.

1. Introduction

Particulate matter (PM), especially with an aerodynamic diameter smaller than 2.5 µm ($PM_{2.5}$), has adverse effects on human health that are commonly presented as respiratory and cardiovascular ailments [1]. It is well known that natural and anthropogenic emissions and meteorological conditions influence ambient $PM_{2.5}$ concentrations. Topography also impacts air quality since it affects the local meteorology [2]. In valleys, cold air can be trapped near the valley floor for more than one day (24 hours) during wintertime with limited insolation, which is known as a persistent cold air pool (PCAP) [3]. PCAP events are characterized by a stably stratified atmospheric boundary layer, calm winds, and low boundary layer height [4]. PCAPs have been documented in multiple valleys and basins in the U.S. [3, 5-8], Asia [9, 10], and Europe [11-13], but the PCAP frequency, strength, and length depends on location. The PCAP strength, characterized by valley heat deficit, is correlated with $PM_{2.5}$ concentrations based on data collected in western U.S. valleys [4, 14, 15].

The Community Multiscale Air Quality (CMAQ) model [16] is a regulatory tool that is used to simulate air quality and is employed in state implementation plans (SIPs) for regulatory planning purposes. There are three main uncertainties associated with chemical transport modeling (CTM): emissions estimates, meteorological modeling, and the model formulation of the atmospheric chemistry processes. Large discrepancies have been identified in global and regional emissions

inventories [17]. A case study in Houston suggested that uncertainties in emissions estimates were associated with uncertainties of 42%~52% in the simulated $PM_{2.5}$ concentrations [18]. Previous studies in U.S. cities have aimed at determining uncertainties in NO_x emissions [19] [20], however there is not a consistent conclusion on whether they are over- or underestimated. To address the discrepancy in NO_x emissions and $PM_{2.5}$ nitrate formation, some studies rely on model tuning, or simply adjusting the emissions rate so that the CMAQ model matches the observed ambient concentrations, which may improve the simulation accuracy but also misrepresent the actual emissions and therefore bias the chemical and physical processes. Emissions tuning is often used for SIPs modeling in the western U.S. where CTMs typically underestimate the elevated wintertime $PM_{2.5}$ concentrations associated with PCAPs [19, 21].

In addition to emission inventories, realistic simulation of the ambient air quality using CMAQ requires accurate meteorological inputs. The meteorology fields are provided by numerical weather prediction models, such as the Weather Research and Forecasting (WRF) model [22]. Crippa et al. [23] found that simulated $PM_{2.5}$ concentrations in the eastern U.S. were sensitive to the selection of the planetary boundary layer (PBL) scheme in WRF as well as the aerosol scheme and emissions inventory. In the western U.S., the PBL scheme is expected to have an even greater impact on the simulated $PM_{2.5}$ concentrations because the mountainous terrain leads to increased uncertainties in WRF, especially during wintertime [24]. Previous studies have investigated whether numerical models can capture the PCAP evolution where the results differ based on the atmospheric scale of interest [25] [26] [27]. In general, these studies found that the large-scale dynamics associated with PCAP initiation and duration were well captured by WRF [10][13]. However, the surface turbulence and boundary layer structure that impact pollutant accumulation and mixing were not well simulated [11][25]. Studies have shown that enhanced vertical resolution

can improve performance in simulating PCAP evolution [27] but not necessarily the decreased turbulent mixing. There is a critical need to better understand the NWP turbulence parameterizations during wintertime air quality events to reliably simulate the air quality [28].

To address this critical need, we evaluate the WRF-CMAQ model performance during PCAP events in the SLV, Utah. Model performance during non-PCAP events is also investigated to understand uncertainties related to emissions estimates and chemistry versus uncertainties related to meteorological conditions. The aims of our study are to understand how well the meteorology fields can be captured by the WRF model, how they impact the CMAQ model performance during PCAPs, and to investigate other possible sources of uncertainty associated with emissions and/or chemistry. Therefore, our simulation time period was selected to focus on a large scale PCAPs field study in the SLV to provide the most complete record of meteorological observations for PCAP events. The discussion provides insights into the potential uncertainties in the NO_x chemistry of the CMAQ model that contributes to simulated $PM_{2.5}$ discrepancies with the aim of providing suggestions for future measurements needed from field campaigns to evaluate the CMAQ model more thoroughly during PCAP events.

2. Material and Methods

2.1 Model configuration

The meteorology fields used to drive the CMAQ model came from the WRF model (v3.7). Four configurations were applied in WRF using different PBL schemes, including the Asymmetric Convective Model version 2 (ACM2) PBL scheme, the Yonsei University (YSU) PBL scheme, the Mellor-Yamada-Janjic (MYJ) and Mellor–Yamada–Nakanishi–Niino (MYNN) schemes. The PBL schemes were paired with their intended surface layer schemes (See Table S1, Supporting Information, SI). The scenario names of model runs are abbreviated using the name of their PBL

schemes, ModACM2, ModYSU, ModMYJ, and ModMYNN. More information on the WRF configurations and model run setup are provided in the SI (Section S1).

To investigate the impacts of PBL schemes on simulated air quality, four sets of CMAQ (v5.2) simulations were performed covering the whole January of 2011, when three strong PCAP events occurred [29]. The outer domain covered the Contiguous United States (CONUS) with 12 km horizontal resolution. The inner domain was centered on the Salt Lake Valley with 4 km horizontal resolution and 41 vertical levels with 20 levels below 1km (Figure S1). Previous studies have demonstrated that the horizontal and vertical resolution impacts the simulated meteorological fields [30], however, CTMs (CMAQ specifically) are more limited in the horizontal resolution than WRF. This is due to the computational power required for the chemistry and physics, and challenges in modeling the finer spatial resolution of the emissions estimates. The emissions were based on the 2011 National Emissions Inventory (NEI) developed by the U.S. Environmental Protection Agency (EPA). CMAQ was configured with the Carbon Bond version 6 gas-phase chemical mechanism [31], AERO6 aerosol module, and aqueous phase chemistry.

2.2 Observational datasets

The Persistent Cold Air Pool Study (PCAPS) provides the observational data of surface meteorology and surface energy fluxes at seven sites, and vertical profiles of temperature and wind speed and laser ceilometer data at National Center for Atmospheric Research (NCAR) Integrated Sounding System (ISS) site located in the SLV (Figure S2). The wintertime field campaign was conducted from December 2010 to February 2011. While the PCAPS field study was one of the largest field campaigns in recent years aimed at quantifying atmospheric processes governing the formation and evolution of PCAP events, there are limited observation data specifically related to the atmospheric chemistry of PCAP events. For this we rely on routinely monitored hourly

observations of gaseous and particulate pollutant concentrations, as well as speciated $PM_{2.5}$ concentrations measured at the Hawthorne site (HW, 49-035-3006; 40.73° N, 111.87° W) from the EPA's Air Quality System (AQS). The Hawthorne site is an EPA NCore (multipollutant) site [32] that also collects filter-based samples every 3rd day for speciated $PM_{2.5}$ as part of the EPA Chemical Speciation Network (CSN) [33]. The U.S. EPA Quality Objectives for measurement data set the precision range of $PM_{2.5}$, NO_x, and O_3 to be ±10%, ±10%, and ±7% respectively [34].

The outputs from CMAQ were paired with observations for evaluation using the Atmospheric Model Evaluation tool (AMET) [35]. The mean bias (MB), mean error (ME), normalized mean bias (NMB), normalized mean error (NME), index of agreement (IOA), and correlation coefficient (r) are calculated to evaluate the model performance for CMAQ. Readers can refer to Kelly et al. [36] and Henneman et al. [37] for reference evaluation statistics.

We use valley heat deficit to determine PCAP periods in the SLV. Valley heat deficit is a bulk measure of the atmospheric stability in the valley and is computed using Eq. 1 [14]:

$$\mathrm{H22} = c_p \int_{sfc}^{2200} \rho(z)[\theta_{2200m} - \theta(z)]dz \qquad \text{(Eq. 1)}$$

where H22 denotes the valley heat deficit from the surface to 2200 m, which is the ridge height of the western boundary of the SLV; c_p is the specific heat of air (J kg^{-1} K^{-1}), sfc is the surface, ρ is air density (kg m^{-3}), θ is the potential temperature (K), and z is the altitude (m). We use the criteria proposed by Whiteman et al. [14] where a PCAP exists when H22 > 4.04 MJ m^{-2} for more than 36 hours.

2.3 Identification of limiting precursor reagent for ammonium nitrate formation

Ammonium nitrate (NH_4NO_3) is the main component of the $PM_{2.5}$ mass during wintertime in northern Utah [38-41]. Identification of the limiting precursor reagent for NH_4NO_3 is needed for

policy makers to make regulations that have effective $PM_{2.5}$ concentration reduction pathways. One method to identify the limiting reagent of NH_4NO_3 is to inspect the aerosol liquid water content (LWC) variation with characteristic aerosol pH [42]. The thermodynamic framework considers the aerosol acidity, aerosol LWC, and temperature (271K in our case). Model simulated aerosol LWC was calculated as the sum of aerosol water for the Aitken and accumulation modes from the CMAQ hourly model raw outputs. The aerosol pH from CMAQ was determined by the ratio of H^+ concentration over the aerosol LWC. Aerosol pH data were excluded when aerosol LWC was below 0.01 μg m^{-3} [43]. By plotting the CMAQ simulated pH versus LWC, the aerosol partitioning fraction can be visualized and compared to the characteristic pH values for ammonium nitrate formation, where four chemical domains can be identified on the plot [42]. Based on the location of the CMAQ pH relative to the characteristic pH, the sensitivity of aerosol formation to NH_3 or HNO_3 can be determined. The four sensitivity regimes for NH_4NO_3 formation are i) NH_3 dominated, ii) HNO_3 dominated, iii) both NH_3 and HNO_3 dominated, and iv) insensitive to both NH_3 and HNO_3, and regimes can be determined based on the location of the datapoints within the chemical domains. The aerosol pH and LWC sensitivity regime plot is discussed in Section 4.

Another method to investigate the limiting reagent of ammonium nitrate formation is the molar ratio of total nitrate (HNO_3(g) + NO_3^-(p)) to total reduced nitrogen (NH_3(g) + NH_4^-(p)) (Eq. 2) [21].

$$\text{Ratio} = \frac{HNO_3(g) + NO_3^-(p)}{NH_3(g) + NH_4^+(p)} \qquad \text{(Eq. 2)}$$

A nitrogen ratio larger than 1 indicates that the limiting reagent for NH_4NO_3 formation is ammonia, and a ratio smaller than 1 indicates that nitric acid is the limiting reagent. This ratio was calculated

using the CMAQ results, and findings are discussed in Section 4 to highlight the model uncertainties related to chemistry and emissions.

3. Results

3.1 Valley heat deficit and vertical profiles

Valley heat deficit is used to measure the CAP strength and has been reported to be correlated with $PM_{2.5}$ in multiple studies [4, 14, 15]. The hourly modeled and observed H22 are shown in Figure 1. Three PCAP events were identified in January 2011 using the hourly sounding observations at the NCAR ISS site based on the aforementioned method (i.e., H22 > 4.04 MJ m^{-2} lasting for more than one day): PCAP1 (1900 MST 1 Jan to 2300 MST 8 Jan), PCAP2 (0500 MST 11 Jan to 0000 MST 14 Jan), and PCAP3 (0300 MST 27 Jan to 1800 MST 30 Jan).

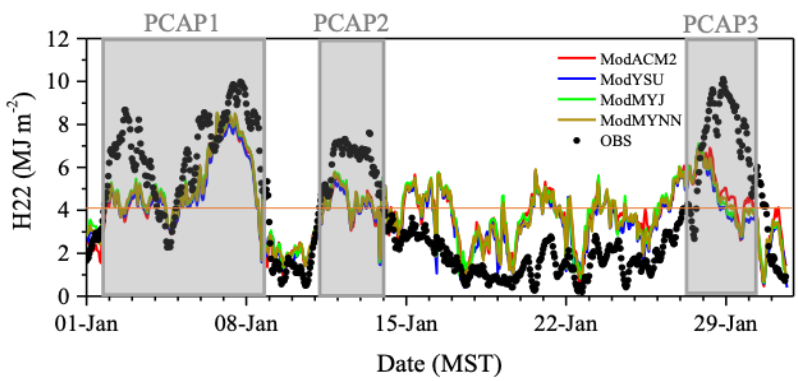

Figure 1 Time series of the hourly simulated valley heat deficit and hourly estimated values from observations at the NCAR ISS site in January 2011. The orange horizontal line indicates the threshold of H22 (4.04 MJ m^{-2}) for a PCAP event.

Compared with observations, the WRF model underestimated H22 during PCAP events and overestimated H22 during non-PCAP periods. The average simulated H22 during PCAP and non-PCAP events was 4.88 MJ m^{-2} and 2.75 MJ m^{-2}, respectively. This indicates that the WRF model is capable of successfully simulating the timing of a PCAP event but cannot accurately simulate the boundary layer bulk stability, i.e. the model simulated less stability during PCAP events and

more stability during non-PCAP events. The inability of the model to simulate the bulk stability under stable boundary layer events is consistent with prior studies [28]. The model simulated less stable atmospheric stratification compared with the ISS site observations during PCAP3 (0300 MST 27 Jan to 1800 MST 30 Jan, Figure S3). Further inspections of the vertical profiles of simulated and observed potential temperature (Figure S4) suggest that WRF simulated less vertical mixing accompanied by a more stably stratified atmosphere, thus higher H22 during non-PCAPs. The four WRF scenarios generated nearly the same H22 values. This implies that the surface $PM_{2.5}$ simulation deficiencies stemming from unrealistic bulk stability (H22) should be similar in the four CMAQ simulations. However, this is not the only determinant meteorological factor, and discrepancies in simulated $PM_{2.5}$ in CMAQ will also result from other predicted meteorological variables, such as temperature and its impact on emissions and chemical reactions. The WRF model performance for other meteorological variables can be found in Figure S4. WRF has also been found to exhibit a positive bias in simulating surface turbulent fluxes during PCAP events [26].

3.2. Gaseous pollutants

Gas-phase pollutants serve as precursors for secondary aerosol formation (e.g., NO_x) and can also directly impact human health (e.g., O_3). Hourly variations of simulated and observed mixing ratios for NO_x and O_3 are illustrated in Figure 2. Analysis of SO_2 simulation results are included in the SI (Figure S6-S8) because it was not the primary species impacting $PM_{2.5}$ concentrations in SLV during PCAPs [38, 44-50]. There were clear day-of-week patterns of NO_x concentrations in the observations, i.e., high on weekdays and low on weekends. The weekly maximum NO_x concentration was enhanced during PCAP events. For example, NO_x levels were elevated during PCAP1 and PCAP2, reaching up to 306 ppb. The CMAQ model was able to

capture the NO_x weekly pattern but not the amplitude. During the non-PCAP period (17 Jan-24 Jan) between PCAP2 and PCAP3, the NO_x levels were overestimated by the model. This is related, in part, to the overestimated H22 accompanied by more stratified potential temperature vertical profiles compared with observations during non-PCAPs, which may simulate higher pollutant concentrations confined in the boundary layer. Modeled NO_x discrepancies may also be related to overestimated NO_x in the emissions inventory, which has also been found by Canty et al. [51]. The observed low NO_x mixing ratios during PCAP3 were related to the low weekend emissions (29 Jan-30 Jan). The high simulated NO_x during PCAP3 implies that the emissions inventory might be overestimating the NO emissions during PCAP3, which is the main contributor to NO_x. The nighttime NO_x underestimations were likely associated with the underestimated H22 during the three PCAP events. Overall, NO_x was overestimated in CMAQ (see Table S2). The ModACM2 run performed best in simulating NO_x with the smallest NMB, ME, and NME.

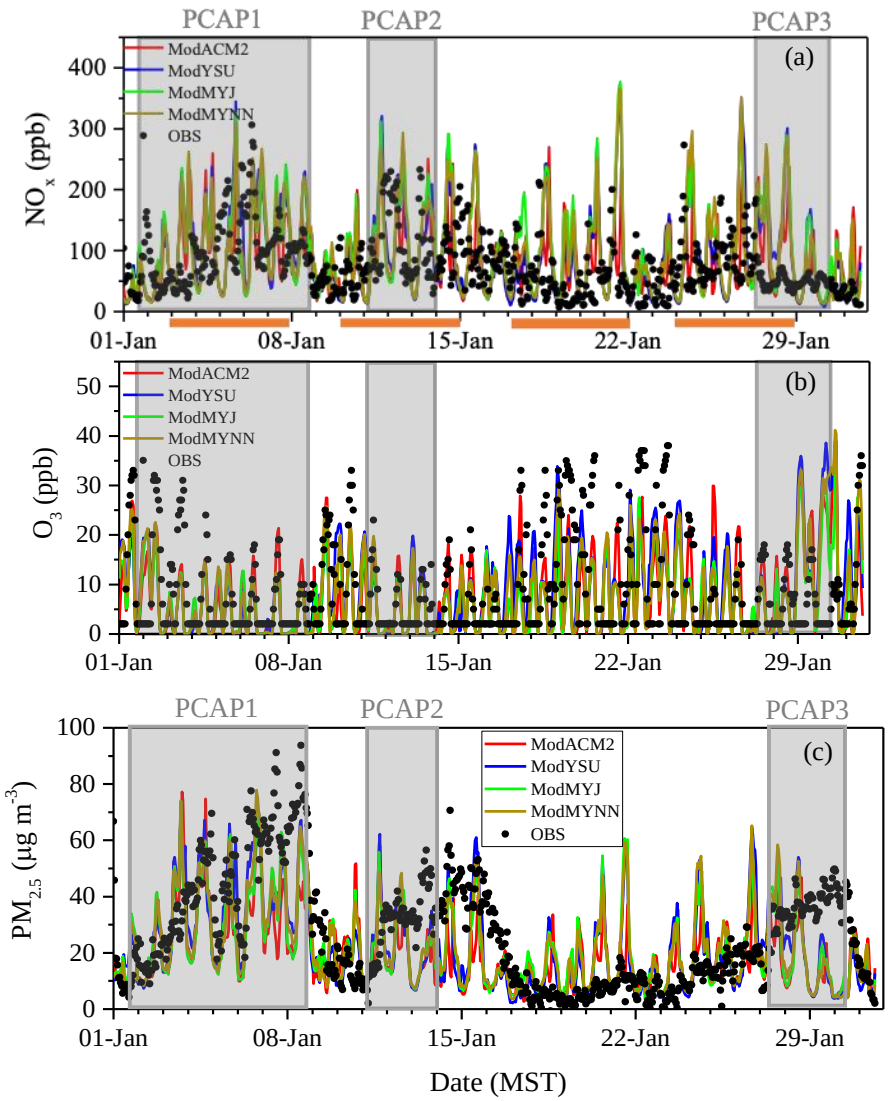

Figure 2 Time series of hourly simulated and observed mixing ratios of (a) NO_x, (b) O_3, and (c) $PM_{2.5}$ at HW site. The nighttime O_3 concentrations reached below the instrument detection limit. The weekdays are indicated with orange bars on the x axis.

The maximum observed O_3 during January was 38 ppb. O_3 had an opposite trend compared to the NO_x since it is titrated through reactions with NO. Higher O_3 was observed during non-PCAPs with less rich NO_x than PCAPs. However, CMAQ simulated lower O_3 accompanied with an underestimation of NO_x for PCAP3. Net radiation was reasonably well-simulated by the WRF model (Figure S5). We suspect the lower O_3 in the CMAQ model might be related to the

modeled photolysis rates during PCAP3. Statistics show that O_3 was underestimated during non-PCAPs (Table S2), which is likely related to the NO_x overestimation during the same time period. The snow cover during PCAP1 contributed to the observed high O_3 concentrations. However, the WRF model underestimated the snow cover [26], and correspondingly simulated less upward shortwave radiation reflected to the atmosphere. Thus, the O_3 concentrations in CMAQ were lower than the observations during PCAP1. The elevated simulated O_3 levels during PCAP3 were partially related to the warmer simulated T2 (Figure S5) compared to observations or unrealistic emissions estimates for the O_3 precursors. The ModMYJ case agreed better with observations in O_3 simulation with a lower ME and NME.

Diel variations of simulated and observed NO_x and O_3 are presented in Figure 3. Observed NO_x concentrations peaked at around 0800 MST and began to increase again after 1600 MST in the non-PCAP scenario, which were partially impacted by fresh on-road emissions. The CMAQ model was able to capture the morning NO_x peak but generated a second peak faster than the observations at around 1800 MST. Observed NO_x exhibited less variation during nighttime during the PCAP case compared with the non-PCAP case. Simulated diel patterns of NO_x concentrations did not change but generated higher peak magnitudes in the PCAP case compared with non-PCAP. Overestimation of NO_x mainly occurred during daytime and underestimation occurred during nighttime. The observed bimodal shape of the O_3 diel distribution with two peaks at around 0400 and 1200 MST in the non-PCAP case were captured by the model but with a lower magnitude. The reason for the O_3 peak in the CMAQ simulations at nighttime might be related to the overestimated downward mixing from above. Observed O_3 remained depleted and nearly constant at nighttime in the PCAP case, which is attributed to the rich NO_x concentrations at the same time.

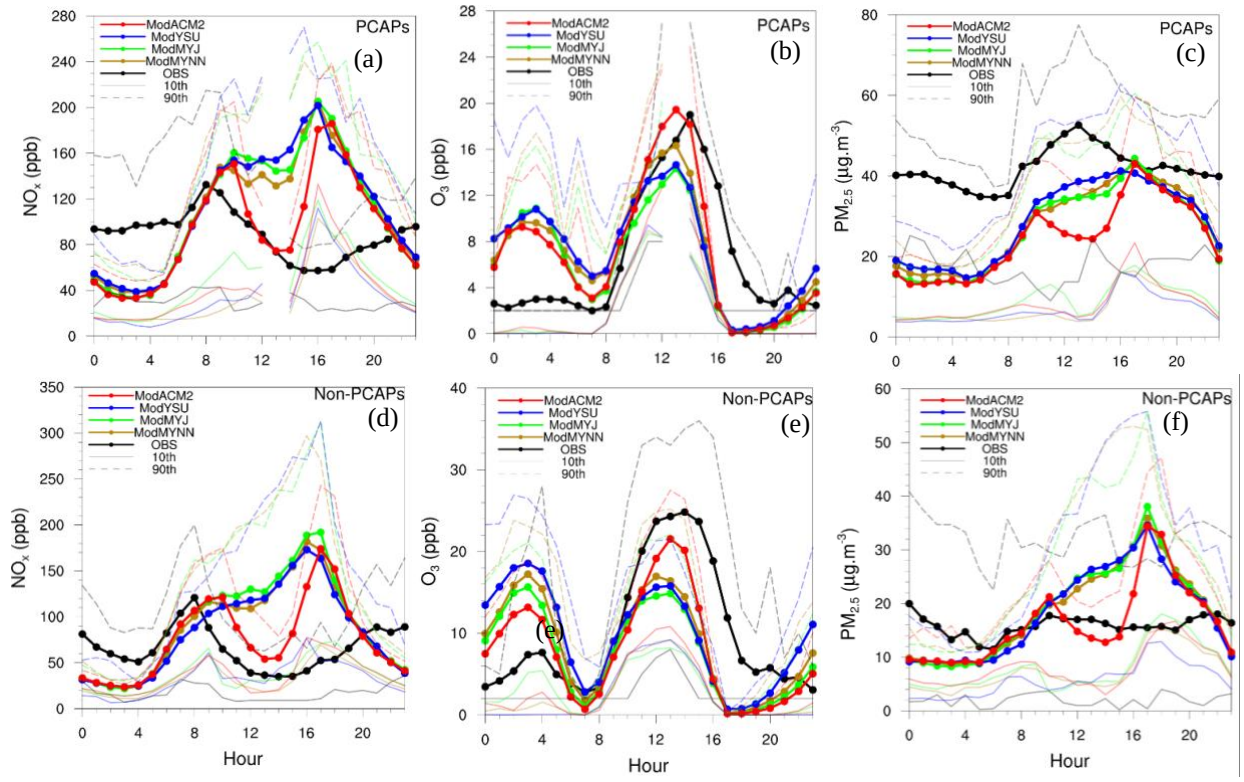

Figure 3 Diel variations of observed and modeled hourly mean values of NO_x, O_3, and $PM_{2.5}$ during PCAP events in (a), (b), and (c), respectively, and non-PCAP events in (d), (e), and (f), respectively. The lower (10th) and upper (90th) decile values are presented for reference by opaque dashed lines and opaque solid lines, respectively. The data gaps in the PCAPs panel are because there are not enough data to plot the lower and upper decile at that time.

In addition to the operational evaluations conducted above, dynamic evaluations were undertaken to determine how much of the pollutant concentration change between PCAP and non-PCAP events are captured by the model. Changes in the mean and percentiles of NO_x, O_3, and $PM_{2.5}$ based on hourly values from observations and the four simulations during PCAPs and non-PCAPs (PCAPs-non-PCAPs) are displayed in Figure 4. Positive (negative) values indicate an increase (decrease) of the concentration during PCAPs compared with non-PCAPs. The results indicate that the mean changes of the two gaseous pollutants were reproduced relatively well by the CMAQ model, including the increase of the NO_x mean, decrease of the O_3 mean, and increase of the SO_2 mean during PCAP events. However, higher deficiencies occurred in simulating the percentile changes, especially for the 90th percentile. The 90th percentile NO_x changes were

underestimated in the simulations, indicating that the model was not able to simulate the large increase in NO_x concentrations during PCAPs compared with non-PCAPs. The 10th and median of observed O_3 changes happen to be zero. The model had mixed performance in simulating the O_3 90th percentile change. This indicates that the model performs well in simulating the overall changes in gaseous species for PCAPs but loses accuracy in simulating high concentration changes. There is no uniform model configuration that performs best for simulating all of the gaseous species and the differences between PCAP and non-PCAP periods.

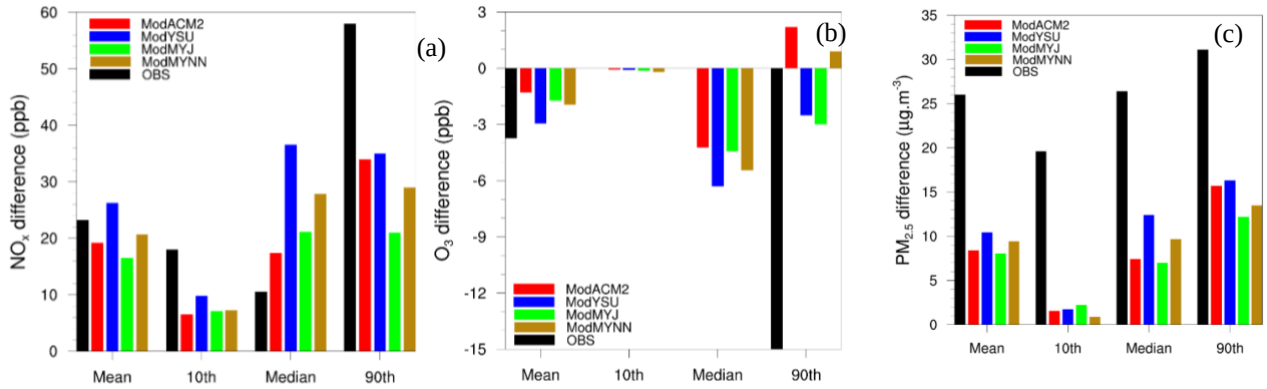

Figure 4 Bar chart of the observed and modeled difference in mean, 10th percentile, median, and 90th percentile of (a) NO_x, (b) O_3, and (c) $PM_{2.5}$ between hourly values during PCAPs and non-PCAPs events (PCAPs-non-PCAPs).

3.3. $PM_{2.5}$

3.3.1 Mass concentration

Comparisons of simulated and observed hourly $PM_{2.5}$ concentrations at the HW site in January are presented in Figure 2(c). Elevated $PM_{2.5}$ concentrations were observed during PCAP events, reaching up to 93.7 μg m^{-3} during PCAP1. This is expected due to the suppressed mixing accompanied by the elevated H22 observed during PCAPs (Figure 1). Overall, the model underestimated (overestimated) $PM_{2.5}$ during PCAP (non-PCAP) events (See Table S3, Supporting Information).

The temporal variations of $PM_{2.5}$ were not well reproduced by the model. The observed daily increase of $PM_{2.5}$ concentrations during PCAP1, PCAP2, and PCAP3 using the daily maximum $PM_{2.5}$ concentrations (Figure S8) at the HW site were 11.5, 11.2, and 4.4 μg m^{-3}/day, respectively. The $PM_{2.5}$ accumulation rate was not captured by the model, where the simulated daily $PM_{2.5}$ concentration increases were 3.5, -3.8, and -8.0 μg m^{-3}/day, respectively for the three PCAP periods.

Observed $PM_{2.5}$ concentrations during PCAP3 were similar in magnitude to PCAP2, although PCAP3 had lower NO_x levels. This is related to the higher observed H22 during PCAP3 compared to PCAP2, which may lead to higher $PM_{2.5}$ concentrations near ground level (i.e., increased stability traps pollutants). The model underestimated H22 during PCAP3 to a larger extent compared to PCAP2. This leads to negative biases in simulated $PM_{2.5}$, despite NO_x being overestimated at the same time. This highlights the importance of realistic simulated meteorology fields in air quality modeling, especially during PCAP events, as well as potential biases in modeled PCAP aerosol formation. Underestimated PCAP strength can lead to underestimated $PM_{2.5}$ concentrations even with overestimated emissions.

Nighttime aerosol nitrate formation and early morning transport has been found to contribute to $PM_{2.5}$ concentration increases during PCAPs based on observations [38] and box models [52]. Diel variations of simulated and observed $PM_{2.5}$ during PCAPs and non-PCAPs are illustrated in Figure 3. Measured $PM_{2.5}$ levels were elevated in PCAPs compared to non-PCAPs during both daytime and nighttime. The observed mean $PM_{2.5}$ values reached a maximum at noon during the PCAPs. Underestimations of $PM_{2.5}$ existed all day with large underestimations occurring at night. There was less diel variability in the $PM_{2.5}$ concentration from observations for the non-PCAPs. The model overestimated $PM_{2.5}$ during daytime and underestimated $PM_{2.5}$ during nighttime. In

addition to the underestimated atmospheric stability, the high observed nighttime $PM_{2.5}$ concentrations were suspected to be related to the nighttime heterogeneous N_2O_5 uptake mechanism for NH_4NO_3 formation that is not well simulated in the CMAQ model.

The $PM_{2.5}$ mean and percentile increases during PCAPs compared with non-PCAPs were captured by the model (Figure 4). However, the magnitudes of the change were largely underestimated. This indicates that the model was able to respond to stably stratified atmospheric boundary layer (ABL) conditions with enhanced pollutant concentrations but with smaller increments compared to observations. Recall that the median NO_x change was overestimated, whereas the median $PM_{2.5}$ change was underestimated. This suggests that in addition to the meteorology fields, the $PM_{2.5}$ simulation deficiencies during PCAPs in CMAQ may also be attributed to chemistry and dry deposition, which are further discussed in Section 4.

3.3.2. Chemical composition

Simulated speciated $PM_{2.5}$ components are compared with observations (Figure 5). The observed $PM_{2.5}$ chemical composition during PCAPs and non-PCAPs both show a large contribution from ammonium and nitrate, 59.1% and 46.6%, respectively. This is consistent with previous studies [38, 53] which found that the percentage of ammonium nitrate increased during inversion cases. The $PM_{2.5}$ concentration increase during PCAP events was largely due to ammonium nitrate. The concentration of observed ammonium nitrate increased from 5.76 μg m^{-3} during non-PCAPs to 25.00 μg m^{-3} during PCAPs.

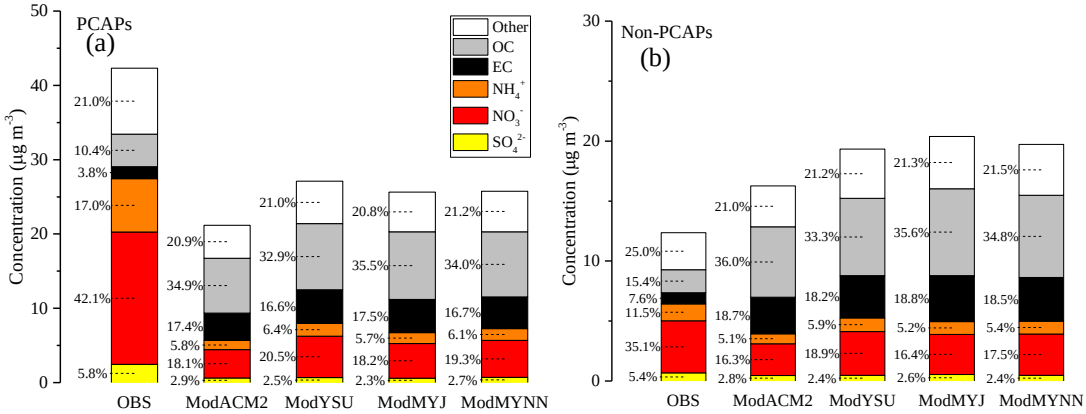

Figure 5 Stacked bar plots of average daily $PM_{2.5}$ chemical composition at the HW site during PCAP events (n=5) and non-PCAP events (n=5).

The CMAQ model simulations produced different $PM_{2.5}$ chemical composition compared to observations (Figure 5). Organic carbon (OC) shows the largest contribution of $PM_{2.5}$ mass concentration in CMAQ followed by nitrate and ammonium, both in PCAPs and non-PCAPs. The simulated ammonium nitrate percentage of the $PM_{2.5}$ mass concentration increased from 22.69% in non-PCAPs to 25.03% in PCAPs. The modeled percentage increase of ammonium and nitrate (2.3%) is not as significant as the observations (12.5%). These results indicate that uncertainties in the chemical processes are also contributing to the underestimated $PM_{2.5}$ concentrations in CMAQ.

4. Discussion

It is well understood that stable boundary layer events, such as PCAPs, can dampen vertical mixing and lead to an accumulation of air pollution concentrations. Discrepancies in simulating atmospheric vertical mixing stem from two sources, one is the initial NWP outputs (WRF), the other is the CTM (CMAQ). In WRF, uncertainties associated with the simulated land-atmosphere interactions, which determine the heat and moisture exchange from the surface to the atmosphere, further impact the simulated boundary layer structure. Sun et al. [26] investigated the surface turbulent fluxes observed during the same field campaign (PCAPS) and found that WRF

overestimated the surface heat fluxes during PCAPs. They found that the surface exchange coefficient, which is a key parameter in simulating surface sensible heat flux, was overestimated in WRF when comparing with values calculated from observational data. Further investigations in Sun et al. [26] show that the flux-profiles adopted by Monin–Obukhov similarity theory that are widely employed in surface layer schemes deviated from the stability function curves estimated from observations. The excessive surface turbulence in the simulations transfers more heat to the boundary layer and leads to higher simulated PBL heights, and thus allows for more vertical mixing and lessens the buildup of air pollution concentrations in the model, similar to our CMAQ findings here.

In CMAQ, some of the meteorological fields are re-processed to generate the specific fields needed in the CTM. One important parameter is the minimum value of eddy diffusivity (Kzmin) which sets a lower bound for the modeled turbulent mixing in CMAQ. This value is currently not available in the WRF outputs. In this study, Kzmin was set to the default 'Y' in the CMAQ configuration, which is a function of urban area fraction in the grid [16]. Kzmin ranges from 0.01 at predominantly non-urban grids to 1 m^2/s at urban grids. The HW site is an urban area and the urban area fraction in the nearest CMAQ grid is 36%. The modeled Kzmin in urban areas can be larger than the actual values in meteorological models [54]. Larger Kzmin in CMAQ tends to smear out the stable boundary layer structure over urban areas and leads to lower simulated air pollutant concentrations under stable atmospheric conditions. A larger Kzmin value would also simulate mixing that brings O_3 from the upper atmosphere with higher concentrations to the surface [54], which partly explains the high nighttime O_3 concentrations (Figure 3c). Regardless of the WRF PBL scheme used, the vertical diffusion within CMAQ is reprocessed using the ACM2 PBL scheme that adopts non-local closure method in the boundary layer. This highlights the

importance of adopting local closure PBL schemes in CTMs, which can be more suitable for stable atmospheric boundary layer conditions compared with non-local closure schemes [26, 30, 55].

In addition, based on previous field campaigns, the chemistry of the secondary aerosol formation that contributes to $PM_{2.5}$ increases in the SLV is still not clear [38, 53, 56]. There have been a limited number of field campaigns aimed at determining the sources of $PM_{2.5}$ increases during winter in the SLV. The Utah Winter Fine Particulate Study (UWFPS) [21] was conducted in the winter of 2015 to 2016 in Northern Utah. UWFPS combined ground-based observations and aircraft measurements to investigate the chemistry process and species important for $PM_{2.5}$ formation. Nocturnal production of ammonium nitrate through the heterogeneous N_2O_5 uptake was found to account for 52%-85% of the morning air pollution accumulation in SLV during winter pollution events using a box model [57]. Using the UWFPS observations, Baasandorj [21] concluded that the formation of ammonium nitrate, which is the main $PM_{2.5}$ component in SLV, was HNO_3 limited using the nitrogen ratio method. However, Womack et al. [58] suggests that NH_4NO_3 formation is insensitive to the NO_x precursor but sensitive to VOCs that can impact oxidation cycles based on photochemical box modeling. Ivey et al. [39] used a source-oriented modeling approach to identify fossil fuel combustion and non-electric generating stationary sources as the top contributors to $PM_{2.5}$ during PCAPs. Here we use the CMAQ model results to further discuss the potential sources contributing to the $PM_{2.5}$ increase during wintertime in SLV.

Model deficiencies for $PM_{2.5}$ stemming from emissions and chemistry are addressed using the thermodynamic ammonium nitrate regime method from Nenes et al. [42]. The CMAQ simulated aerosol pH and simulated aerosol LWC from the four model scenarios are shown in Figure 6. The simulated aerosol pH in SLV for Jan 2011 was below 3, with a few exceptions above 3 and below 5 in Mod_YSU and Mod_MYNN. This indicates that there are acidic aerosol conditions in SLV

during wintertime. The pH range at the low $PM_{2.5}$ concentration end is higher than at the high $PM_{2.5}$ end. The characteristic pH and LWC curves were calculated based on the average temperature during Jan 2011 (271K) using the spreadsheet in the supplemental material from Nenes et al. [42]. Based on this aerosol pH and LWC method, most of the data points reside in the NH_3 sensitive region. This means that there are high enough HNO_3 concentrations that the aerosol formation is not limited by HNO_3 but by NH_3, indicating that SLV is in the NH_3-dominated regime. With increasing $PM_{2.5}$ concentration above ~15 μg m^{-3}, the data points move to the HNO_3-NH_3 sensitive region. The transition of the sensitivity regime from NH_3 to HNO_3-NH_3 in Figure 6 is suspected to be governed by the LWC variations. High aerosol LWC promotes more PM formation because it enhances the sensitivity of aerosols to NH_3 and HNO_3 levels. Mapping the LWC and RH (Figure S10) shows that higher LWC is associated with higher RH.

The aerosol pH and LWC can also regulate the dry deposition of nitrogen, impacting the simulated $PM_{2.5}$ nitrate concentrations. Nenes et al. [59] found that conditions that favor a high partitioning fraction of nitrate (e.g., high RH) reduce the dry deposition velocity, which allows for the accumulation of nitrate aerosol. The lower simulated RH (MB= -18%) from WRF during the three PCAP events contributes less aerosol formation, as well as higher dry deposition rates. Both would lead to underestimated $PM_{2.5}$ in the CMAQ simulation results because of the underestimated nitrate (i.e., less nitrate formation and increased nitrogen deposition).

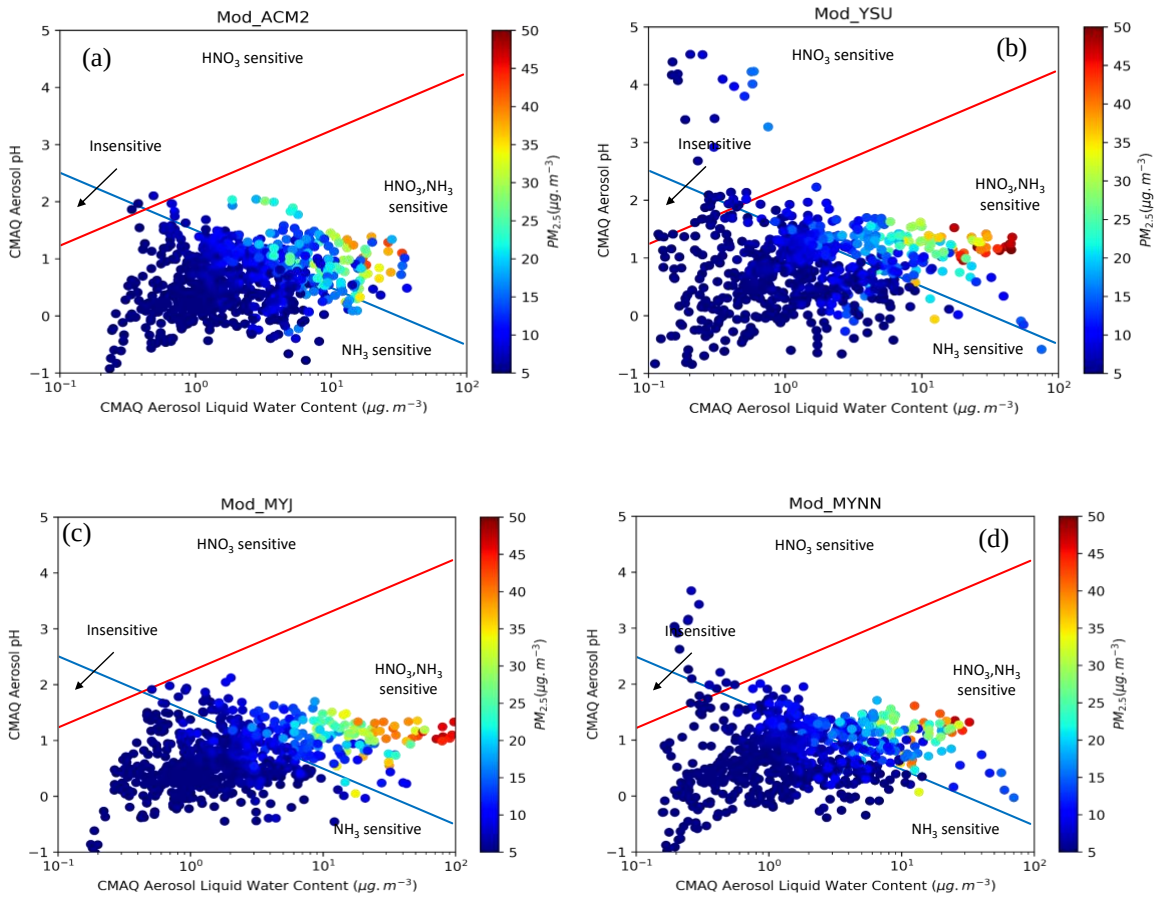

Figure 6 CMAQ simulated aerosol pH variations with simulated aerosol liquid water content from (a) Mod_ACM2, (b) Mod_YSU, (c) Mod_MYJ, and (d) Mod_MYNN. The datapoints are color-coded by $PM_{2.5}$ concentration. The blue line and red line are the characteristic pH to define when aerosol is sensitive to changes in available nitrate and ammonia, respectively.

Using the nitrogen ratio method, the simulated limiting reagents for ammonium nitrate variation with $PM_{2.5}$ are shown in Figure S11, SI. The simulated nitrogen ratio was less than 1, except for five datapoints. This suggests that the NH_4NO_3 formation in SLV during wintertime was mainly in excess of reduced nitrogen and limited by HNO_3(g). This was also demonstrated by observations from the UWFPS [21] and measurements collected during two inversion events during wintertime in 2009 [53]. The nitrogen ratio method contradicts the results based on the PM

sensitivity to HNO_3 and NH_3 discussed above. This indicates the equilibrium of ammonium nitrate is not simply expressed by a balance between HNO_3/NO_3- and NH_3/NH_4^+.

The model also simulated a decreasing nitrogen ratio with increasing $PM_{2.5}$ concentrations. This indicates that NH_4NO_3 formation became more HNO_3(g) limited with higher concentrations of $PM_{2.5}$ in the simulations. However, Baasandorj [21] reported larger nitrogen ratios (close to 1) under high aerosol loadings, although with a limited number of observations. They suggested that the ammonium nitrate formation shifted to NH_3-limited with time during long PCAP episodes based on observations. This reverse behavior of the variation of nitrogen ratio with increasing $PM_{2.5}$ concentrations in CMAQ suggests that the model may underestimate nitric acid formation during pollution episodes associated with PCAP events, as ratios less than one indicate higher reduced nitrogen in the model and nitrate concentrations were greater than ammonium concentrations. This is possibly related to the nighttime nitrate formation through N_2O_5 heterogeneous reactions that are not well addressed in models [19, 38]. It is also important to note that the observation results in Baasandorj [21] were for PM_1, while our CMAQ simulations are for $PM_{2.5}$. Further inspection shows that the CMAQ simulated nitrogen ratio for PM_1 exhibited similar magnitudes and trends compared to $PM_{2.5}$ (Figure S9).

More effort, including both measurements and model development, is needed to understand the aerosol nitrate formation mechanism during wintertime air pollution events, particularly in mountainous regions. Future field campaigns aiming to improve the understanding of increased wintertime $PM_{2.5}$ concentrations should be comprehensive in considering the complexity of the aerosol formation and transport. It is pivotal that a field campaign includes thorough measurements focusing on both meteorology and chemistry. Surface sensible heat fluxes, which transfer heat from the surface to the boundary layer, have been found to be overestimated during PCAPs [26].

Eddy covariance flux tower measurements to study the land-atmosphere exchange during the stable boundary layer events can help understand the atmospheric physics during PCAP evolution, thus contributing to improved parameterizations of land-atmosphere interactions and turbulent mixing in NWP models. In addition to the routine concentration measurements of $PM_{2.5}$, high temporal resolution (hourly or shorter) of speciated $PM_{2.5}$ concentrations and gas phase precursors during both daytime and nighttime can provide valuable information, in particular for nighttime ammonium nitrate formation and transport. Vertical measurements of these meteorology and chemistry variables should be combined with ground-based observations to help understand the PCAP evolution and aerosol formation and transport.

Acknowledgements

Xia Sun is supported in part by the NOAA Cooperative Agreement with CIRES, NA17OAR4320101. We would like to thank Havala Pye from the U.S. Environmental Protection Agency for providing information regarding to CMAQ aerosol pH and LWC calculation.

Supporting Information

The supporting information includes: WRF Model Setup (Section S1), Vertical Profiles of Temperature and Aerosol Backscatter (Section S2), SO_2 Simulation Analysis (Section S3), 2 tables and 11 figures.

References

1. Wallace, J., P. Nair, and P. Kanaroglou, *Atmospheric remote sensing to detect effects of temperature inversions on sputum cell counts in airway diseases.* Environmental Research, 2010. **110**(6): p. 624-632.
2. Wallace, J., D. Corr, and P. Kanaroglou, *Topographic and spatial impacts of temperature inversions on air quality using mobile air pollution surveys.* Science of The Total Environment, 2010. **408**(21): p. 5086-5096.
3. Whiteman, C.D., S. Zhong, W.J. Shaw, J.M. Hubbe, X. Bian, and J. Mittelstadt, *Cold Pools in the Columbia Basin.* Weather and Forecasting, 2001. **16**(4): p. 432-447.

4. Silcox, G.D., K.E. Kelly, E.T. Crosman, C.D. Whiteman, and B.L. Allen, *Wintertime PM2.5 concentrations during persistent, multi-day cold-air pools in a mountain valley.* Atmospheric Environment, 2012. **46**: p. 17-24.
5. Bares, R., J.C. Lin, S.W. Hoch, M. Baasandorj, D.L. Mendoza, B. Fasoli, L. Mitchell, D. Catharine, and B.B. Stephens, *The Wintertime Covariation of CO2 and Criteria Pollutants in an Urban Valley of the Western United States.* Journal of Geophysical Research: Atmospheres, 2018. **123**(5): p. 2684-2703.
6. Clements, C.B., C.D. Whiteman, and J.D. Horel, *Cold-Air-Pool Structure and Evolution in a Mountain Basin: Peter Sinks, Utah.* Journal of Applied Meteorology, 2003. **42**(6): p. 752-768.
7. Billings, B.J., V. Grubišić, and R.D. Borys, *Maintenance of a Mountain Valley Cold Pool: A Numerical Study.* Monthly Weather Review, 2006. **134**(8): p. 2266-2278.
8. Chemel, C., G. Arduini, C. Staquet, Y. Largeron, D. Legain, D. Tzanos, and A. Paci, *Valley heat deficit as a bulk measure of wintertime particulate air pollution in the Arve River Valley.* Atmospheric Environment, 2016. **128**: p. 208-215.
9. Wang, J., Y. Wang, H. Liu, Y. Yang, X. Zhang, Y. Li, Y. Zhang, and G.J.A.E. Deng, *Diagnostic identification of the impact of meteorological conditions on PM2. 5 concentrations in Beijing.* 2013. **81**: p. 158-165.
10. Cao, B., S. Gruber, and T.J.G.M.D. Zhang, *REDCAPP (v1. 0): Parameterizing valley inversions in air temperature data downscaled from reanalyses.* 2017. **10**(8): p. 2905-2923.
11. Pagès, M., N. Pepin, and J.R. Miró, *Measurement and modelling of temperature cold pools in the Cerdanya valley (Pyrenees), Spain.* Meteorological Applications, 2017. **24**(2): p. 290-302.
12. Dorninger, M., C.D. Whiteman, B. Bica, S. Eisenbach, B. Pospichal, and R. Steinacker, *Meteorological Events Affecting Cold-Air Pools in a Small Basin.* Journal of Applied Meteorology and Climatology, 2011. **50**(11): p. 2223-2234.
13. Quimbayo-Duarte, J., C. Chemel, C. Staquet, F. Troude, and G.J.A.E. Arduini, *Drivers of severe air pollution events in a deep valley during wintertime: A case study from the Arve river valley, France.* 2021. **247**: p. 118030.
14. Whiteman, C.D., S.W. Hoch, J.D. Horel, and A. Charland, *Relationship between particulate air pollution and meteorological variables in Utah's Salt Lake Valley.* Atmospheric Environment, 2014. **94**: p. 742-753.
15. Green, M.C., J.C. Chow, J.G. Watson, K. Dick, and D. Inouye, *Effects of Snow Cover and Atmospheric Stability on Winter PM2.5 Concentrations in Western U.S. Valleys.* Journal of Applied Meteorology and Climatology, 2015. **54**(6): p. 1191-1201.
16. US EPA Office of Research and Development, *CMAQ*. 2017, Zenodo.
17. Granier, C., B. Bessagnet, T. Bond, A. D'Angiola, H.D. van Der Gon, G.J. Frost, A. Heil, J.W. Kaiser, S. Kinne, and Z.J.C.C. Klimont, *Evolution of anthropogenic and biomass burning emissions of air pollutants at global and regional scales during the 1980–2010 period.* 2011. **109**(1): p. 163-190.
18. Zhang, W., M.A. Trail, Y. Hu, A. Nenes, and A.G.J.A.E. Russell, *Use of high-order sensitivity analysis and reduced-form modeling to quantify uncertainty in particulate matter simulations in the presence of uncertain emissions rates: A case study in Houston.* 2015. **122**: p. 103-113.
19. McKeen, S.A., W.M. Angevine, B. McDonald, R. Ahmadov, A. Franchin, A.M. Middlebrook, D.L. Fibiger, E.E. McDuffie, C. Womack, and S.S. Brown. *Modeling of*

meteorology, chemistry and aerosol for the 2017 Utah Winter Fine Particle Study. in *AGU Fall Meeting Abstracts*. 2017.

20. Tong, D.Q., L. Lamsal, L. Pan, C. Ding, H. Kim, P. Lee, T. Chai, K.E. Pickering, and I. Stajner, *Long-term NOx trends over large cities in the United States during the great recession: Comparison of satellite retrievals, ground observations, and emission inventories.* Atmospheric Environment, 2015. **107**: p. 70-84.
21. Baasandorj, M., *Final Report for Utah Winter Fine Particulate Study (UWFPS)*. 2018.
22. Skamarock, W.C., J.B. Klemp, J. Dudhia, D.O. Gill, D.M. Barker, W. Wang, and J.G. Powers, *A description of the Advanced Research WRF version 3. NCAR Technical note-475+ STR.* 2008.
23. Crippa, P., R. Sullivan, A. Thota, and S.J.J.o.G.R.A. Pryor, *Sensitivity of simulated aerosol properties over eastern North America to WRF -Chem parameterizations.* 2019. **124**(6): p. 3365-3383.
24. Sun, X., H.A. Holmes, and H. Xiao, *Surface Turbulent Fluxes during Persistent Cold Air Pool Events in the Salt Lake Valley, Utah. Part II: Simulations.* 2020. **0**(0): p. null.
25. Wei, L., Z. Pu, and S. Wang, *Numerical Simulation of the Life Cycle of a Persistent Wintertime Inversion over Salt Lake City.* Boundary-Layer Meteorology, 2013. **148**(2): p. 399-418.
26. Sun, X., H.A. Holmes, and H. Xiao, *Surface Turbulent Fluxes during Persistent Cold Air Pool Events in the Salt Lake Valley, Utah. Part II: Simulations.* Journal of Applied Meteorology and Climatology, 2020. **59**(6): p. 1029-1050.
27. Vosper, S., E. Carter, H. Lean, A. Lock, P. Clark, and S. Webster, *High resolution modelling of valley cold pools.* Atmospheric Science Letters, 2013. **14**(3): p. 193-199.
28. Baker, K.R., H. Simon, and J.T. Kelly, *Challenges to modeling "cold pool" meteorology associated with high pollution episodes*. 2011, Environmental Sciencce & Technology. p. 7118-7119.
29. Lareau, N.P., E. Crosman, C.D. Whiteman, J.D. Horel, S.W. Hoch, W.O.J. Brown, and T.W. Horst, *The Persistent Cold-Air Pool Study.* Bulletin of the American Meteorological Society, 2013. **94**(1): p. 51-63.
30. Sun, X., H.A. Holmes, O.O. Osibanjo, Y. Sun, and C.E. Ivey, *Evaluation of surface fluxes in the WRF Model: Case study for farmland in rolling terrain.* Atmosphere, 2017. **8**(10): p. 197.
31. Yarwood, G., G. Whitten, J. Jung, G. Heo, and D. Allen, *Development, evaluation and testing of version 6 of the carbon Bond chemical mechanism (CB6).* Final Report prepared for Texas Commission on Environmental Quality, September, 2010.
32. U.S. Environmental Protection Agency. *NCore Monitoring Network*. 2020 [cited 2021 June 14]; Available from: https://www.epa.gov/amtic/ncore-monitoring-network.
33. U.S. Environmental Protection Agency. *Chemical Speciation Network (CSN)*. 2021 [cited 2021 June 14]; Available from: https://www.epa.gov/amtic/chemical-speciation-network-csn.
34. standards, U.S.E.O.o.A.Q.P.a., *Quality Assurance Handbook for Air Pollution Measurement Systems Volume II Ambient Air Quality Monitoring Program*. 2017.
35. Appel, K.W., R.C. Gilliam, N. Davis, A. Zubrow, and S.C. Howard, *Overview of the atmospheric model evaluation tool (AMET) v1.1 for evaluating meteorological and air quality models.* Environmental Modelling & Software, 2011. **26**(4): p. 434-443.

36. Kelly, J.T., S.N. Koplitz, K.R. Baker, A.L. Holder, H.O. Pye, B.N. Murphy, J.O. Bash, B.H. Henderson, N.C. Possiel, and H. Simon, *Assessing PM2. 5 model performance for the conterminous US with comparison to model performance statistics from 2007-2015.* Atmospheric Environment, 2019. **214**: p. 116872.
37. Henneman, L.R., C. Liu, Y. Hu, J.A. Mulholland, and A.G. Russell, *Air quality modeling for accountability research: Operational, dynamic, and diagnostic evaluation.* Atmospheric Environment, 2017. **166**: p. 551-565.
38. Baasandorj, M., S.W. Hoch, R. Bares, J.C. Lin, S.S. Brown, D.B. Millet, R. Martin, K. Kelly, K.J. Zarzana, and C.D. Whiteman, *Coupling between chemical and meteorological processes under persistent cold-air pool conditions: Evolution of wintertime PM2. 5 pollution events and N2O5 observations in Utah's Salt Lake Valley.* Environmental science & technology, 2017. **51**(11): p. 5941-5950.
39. Ivey, C.E., S. Balachandran, S. Colgan, Y. Hu, and H.A. Holmes, *Investigating fine particulate matter sources in Salt Lake City during persistent cold air pool events.* Atmospheric Environment, 2019. **213**: p. 568-578.
40. Kelly, K.E., R. Kotchenruther, R. Kuprov, and G.D. Silcox, *Receptor model source attributions for Utah's Salt Lake City airshed and the impacts of wintertime secondary ammonium nitrate and ammonium chloride aerosol.* Journal of the Air & Waste Management Association, 2013. **63**(5): p. 575-590.
41. Eatough, D.J., T. Cruickshank, N. Olson, P.M. Cropper, and J.C. Hansen, *Composition and secondary formation of fine particulate matter in the Salt Lake Valley: Winter 2009 AU - Kuprov, Roman.* Journal of the Air & Waste Management Association, 2014. **64**(8): p. 957-969.
42. Nenes, A., S.N. Pandis, R.J. Weber, and A. Russell, *Aerosol pH and liquid water content determine when particulate matter is sensitive to ammonia and nitrate availability.* Atmos. Chem. Phys., 2020. **20**(5): p. 3249-3258.
43. Pye, H.O., A. Nenes, B. Alexander, A.P. Ault, M.C. Barth, S.L. Clegg, J.L. Collett Jr, K.M. Fahey, C.J. Hennigan, and H.J.U.F.C. Herrmann, *The acidity of atmospheric particles and clouds.* 2019.
44. Wen, Z., W. Xu, X. Pan, M. Han, C. Wang, K. Benedict, A. Tang, J.L. Collett Jr, and X. Liu, *Effects of reactive nitrogen gases on the aerosol formation in Beijing from late autumn to early spring.* Environmental Research Letters, 2021. **16**(2): p. 025005.
45. Wang, H., X. Wang, H. Zhou, H. Ma, F. Xie, X. Zhou, Q. Fan, C. Lü, and J. He, *Stoichiometric characteristics and economic implications of water-soluble ions in PM2. 5 from a resource-dependent city.* Environmental Research, 2021. **193**: p. 110522.
46. Hrdina, A., J.G. Murphy, A.G. Hallar, J.C. Lin, A. Moravek, R. Bares, R.C. Petersen, A. Franchin, A.M. Middlebrook, and L. Goldberger, *The Role of Coarse Aerosol Particles as a Sink of HNO 3 in Wintertime Pollution Events in the Salt Lake Valley.* Atmospheric Chemistry and Physics Discussions, 2020: p. 1-27.
47. Pétron, G., B. Miller, B. Vaughn, E. Thorley, J. Kofler, I. Mielke-Maday, O. Sherwood, E. Dlugokencky, B. Hall, and S. Schwietzke, *Investigating large methane enhancements in the US San Juan Basin.* Elementa: Science of the Anthropocene, 2020. **8**(1).
48. Kikaj, D., S.D. Chambers, M. Kobal, J. Crawford, and J. Vaupotič, *Characterizing atmospheric controls on winter urban pollution in a topographic basin setting using Radon-222.* Atmospheric Research, 2020. **237**: p. 104838.

49. Liu, Y. and F. Dong, *Corruption, economic development and haze pollution: Evidence from 139 global countries.* Sustainability, 2020. **12**(9): p. 3523.
50. Zhang, Q., T. Gao, X. Liu, and Y. Zheng, *Public environment emotion prediction model using LSTM network.* Sustainability, 2020. **12**(4): p. 1665.
51. Canty, T.P., L. Hembeck, T.P. Vinciguerra, D.C. Anderson, D.L. Goldberg, S.F. Carpenter, D.J. Allen, C.P. Loughner, R.J. Salawitch, and R.R. Dickerson, *Ozone and NOx chemistry in the eastern US: evaluation of CMAQ/CB05 with satellite (OMI) data.* Atmos. Chem. Phys., 2015. **15**(19): p. 10965-10982.
52. McDuffie, E.E., D.L. Fibiger, W.P. Dubé, F. Lopez-Hilfiker, B.H. Lee, J.A. Thornton, V. Shah, L. Jaeglé, H. Guo, R.J. Weber, J. Michael Reeves, A.J. Weinheimer, J.C. Schroder, P. Campuzano-Jost, J.L. Jimenez, J.E. Dibb, P. Veres, C. Ebben, T.L. Sparks, P.J. Wooldridge, R.C. Cohen, R.S. Hornbrook, E.C. Apel, T. Campos, S.R. Hall, K. Ullmann, and S.S. Brown, *Heterogeneous N2O5 Uptake During Winter: Aircraft Measurements During the 2015 WINTER Campaign and Critical Evaluation of Current Parameterizations.* Journal of Geophysical Research: Atmospheres, 2018. **123**(8): p. 4345-4372.
53. Kuprov, R., D.J. Eatough, T. Cruickshank, N. Olson, P.M. Cropper, and J.C. Hansen, *Composition and secondary formation of fine particulate matter in the Salt Lake Valley: Winter 2009.* Journal of the Air & Waste Management Association, 2014. **64**(8): p. 957-969.
54. Li, X. and B.J.A.E. Rappenglueck, *A study of model nighttime ozone bias in air quality modeling.* 2018. **195**: p. 210-228.
55. Hu, X.-M., J.W. Nielsen-Gammon, and F. Zhang, *Evaluation of three planetary boundary layer schemes in the WRF model.* Journal of Applied Meteorology and Climatology, 2010. **49**(9): p. 1831-1844.
56. Hrdina, A., J.G. Murphy, A.G. Hallar, J.C. Lin, A. Moravek, R. Bares, R.C. Petersen, A. Franchin, A.M. Middlebrook, L. Goldberger, B.H. Lee, M. Baasandorj, and S.S. Brown, *The role of coarse aerosol particles as a sink of HNO3 in wintertime pollution events in the Salt Lake Valley.* Atmos. Chem. Phys., 2021. **21**(10): p. 8111-8126.
57. Moravek, A., J.G. Murphy, A. Hrdina, J.C. Lin, C. Pennell, A. Franchin, A.M. Middlebrook, D.L. Fibiger, C.C. Womack, E.E.J.A.C. McDuffie, and Physics, *Wintertime spatial distribution of ammonia and its emission sources in the Great Salt Lake region.* 2019. **19**(24): p. 15691.
58. Womack, C., E. McDuffie, P. Edwards, R. Bares, J. de Gouw, K. Docherty, W. Dubé, D. Fibiger, A. Franchin, and J.J.G.R.L. Gilman, *An odd oxygen framework for wintertime ammonium nitrate aerosol pollution in urban areas: NOx and VOC control as mitigation strategies.* 2019. **46**(9): p. 4971-4979.
59. Nenes, A., S.N. Pandis, M. Kanakidou, A.G. Russell, S. Song, P. Vasilakos, and R.J. Weber, *Aerosol acidity and liquid water content regulate the dry deposition of inorganic reactive nitrogen.* Atmospheric Chemistry and Physics, 2021. **21**(8): p. 6023-6033.